Scientific Research Publishing

Open Journal of Metal, 2019, 9, 33-41
https://www.scirp.org/journal/ojmetal
ISSN Online: 2164-277X
ISSN Print: 2164-2761

Synthesis of Polymer Blend Ferrite Composite for Microwave Absorption at X-Band Frequency

Pukhrambam Dipak, Dinesh Chandra Tiwari, Shailendra Kumar Dwivedi

School of Studies in Physics, Jiwaji University, Gwalior, India
Email: pukchaokhuman@gmail.com, dctiwar2001@yahoo.com

How to cite this paper: Dipak, P., Tiwari, D.C. and Dwivedi, S.K. (2019) Synthesis of Polymer Blend Ferrite Composite for Microwave Absorption at X-Band Frequency. *Open Journal of Metal*, **9**, 33-41.
https://doi.org/10.4236/ojmetal.2019.94004

Received: December 17, 2019
Accepted: December 27, 2019
Published: December 30, 2019

Abstract

The microwave absorption properties of polymer composite PANI/PVA/$NiFe_2O_3$ are investigated. The polymer composites of PANI/PVA and $NiFe_2O_3$ are prepared in two steps. $NiFe_2O_3$ is synthesized by modified sol gel method and PANI by chemical polymerization method. Microwave absorption parameters of polymer composite are measured at X-band. The microwave absorption is found to be −28 dB (99%) at 10.2 GHz. Different characterization techniques such as SEM-EDX, FTIR and XRD are done. The SEM result shows flakes like structure for PANI/PVA and crystalline structure for $NiFe_2O_3$. FTIR of the composite reveals the interaction between the PANI/PVA and $NiFe_2O_3$.

Keywords

Chemical Polymerization, Microwave, Permittivity, Permeability, Reflection Loss, Sol Gel

1. Introduction

Electromagnetic interference became very serious problem in the modern day microwaves communication. Microwave affects the neuron electrical conductivity leading to long term neurological disorder in humans [1]. In order to minimize these problems new materials are synthesized having the potential to absorb or shield the microwave. Microwave absorbing materials (MAM) also play an important role in the military defence system in application to RADAR. Various techniques are used for synthesizing the materials. These materials are magnetic, non-magnetic or composite of both with conducting polymer magnetic. Conducting polymer polyaniline can be synthesized by chemically or by electrochemical polymerization [2]. Ferrites based materials have high coercive force, reliable magnetization, large magneto-crystalline anisotropy, chemical

stability and low cost [3] [4] [5]. They are used in various devices like core of the transformer, microwave and magnetic memories, noise filter [6] and photodegradation [7] [8] [9] [10]. Nickel Ferrite is considered to be n-types semiconductor. The complex part of the permittivity (ε'') and permeability (μ'') are directly associated with the microwave absorption. Microwave absorbing materials should be light weight, chemically and environmentally stable and low density. Jin *et al.* synthesized PPy/MMT polymer composite, which has the microwave absorbing power of −10 dB at X-band frequency [11]. Tiwari [12] *et al.* developed a simple differential bridge technique to measure the dielectric constant of thin polymer film of PPy and polystyrene at microwave range. The results are in good agreement with the reported data. PPy/TiO_2(np)/CNT and PANI/TiO_2(np)-Fe^{3+} polymer nanocomposite have the microwave absorption of 99.99% [13] [14]. Composite of conducting polymer and magnetic material will give better absorption.

The synthesized polymer nanocomposite material has the minimum reflection loss of −28 dB which is 99% adsorption at 10.2 GHz. The magnetic loss inside the material was responsible for the microwave adsorption by the material.

2. Experimental Method

Nickel ferrite material is synthesized by using a modified sol gel method. Analytical grade $Fe(NO_3)_3{\cdot}9H_2O$ and $Ni(NO_3)_3{\cdot}6H_2O$ are taken in a 2:1 molar ratio, dissolved in ethylene glycol at room temperature and is sonicated for 30 min. 3 M of citric acid is added to homogenize the metal ions present in the solution. The solution is heated at 60˚C for 2 hr to form a wet gel and this is further calcinited at 600˚C leading to auto-ignition to produce fluffy nickel ferrite. H_2SO_4 (0.1 M) and aniline (ANI) 0.1 M is dissolved in 50 ml of de-ionize water (DI). Pre-prepared polyvinyl alcohol (PVA) 1.4 mM solution and nickel ferrite is added to ANI/H_2SO_4 solution and stirrered for 1 hr. Ammonium peroxydisulfate (APS) 0.1 M dissolve in water is added drop wise to the solution. And finally it is left for chemical polymerization at 10˚C. The polymer nanocomposite is filtered and washed with DI water several times and dried at 60˚C. The polymer composite is palletized by hydraulic press for different thickness of 2 mm, 2.25 mm, 2.5 mm and 2.95 mm respectively. Finally, we tested for microwave absorption at X-band frequency for the samples.

3. Characterization

The synthesized polymer nanocomposite is characterized by the SEM-EDX, FITR and XRD. The electromagnetic parameters such as permittivity, permeability and reflection loss are measured by using vector network analyzer (Agilent ENA 50 GHz) between frequencies 8 - 12 GHz.

4. Result and Discussion

4.1. SEM-EDX, FTIR and XRD Study

The SEM image of the polymer nanocomposite in **Figure 1(a)** shows the forma-

tion of $NiFe_2O_3$ crystal and polyaniline/PVA flake like structures. The elemental composition of PANI/PVA/$NiFe_2O_3$ is shown in **Figure 1(d)** by EDX. The elemental compositions are given in **Table 1**. The FTIR spectrum of polymer composite is shown in **Figure 1(c)**. The characteristic peak at the 1540 cm^{-1}, 985 cm^{-1}, 1050 cm^{-1}, 1290 cm^{-1} are due to the C=C stretching, N=Q=N (Q = quionoid ring), C=C stretching mode in benzenoid ring and C-N stretching. The peak at the 600 cm^{-1} shows the interaction between the PANI/PVA and $NiFe_2O_3$ [15].

Figure 1(b) shows the powder XRD of the PANI/PVA/$NiFe_2O_3$, to investigate the crystallinity of the sample. We have found the three peaks at 18.96˚, 30˚,

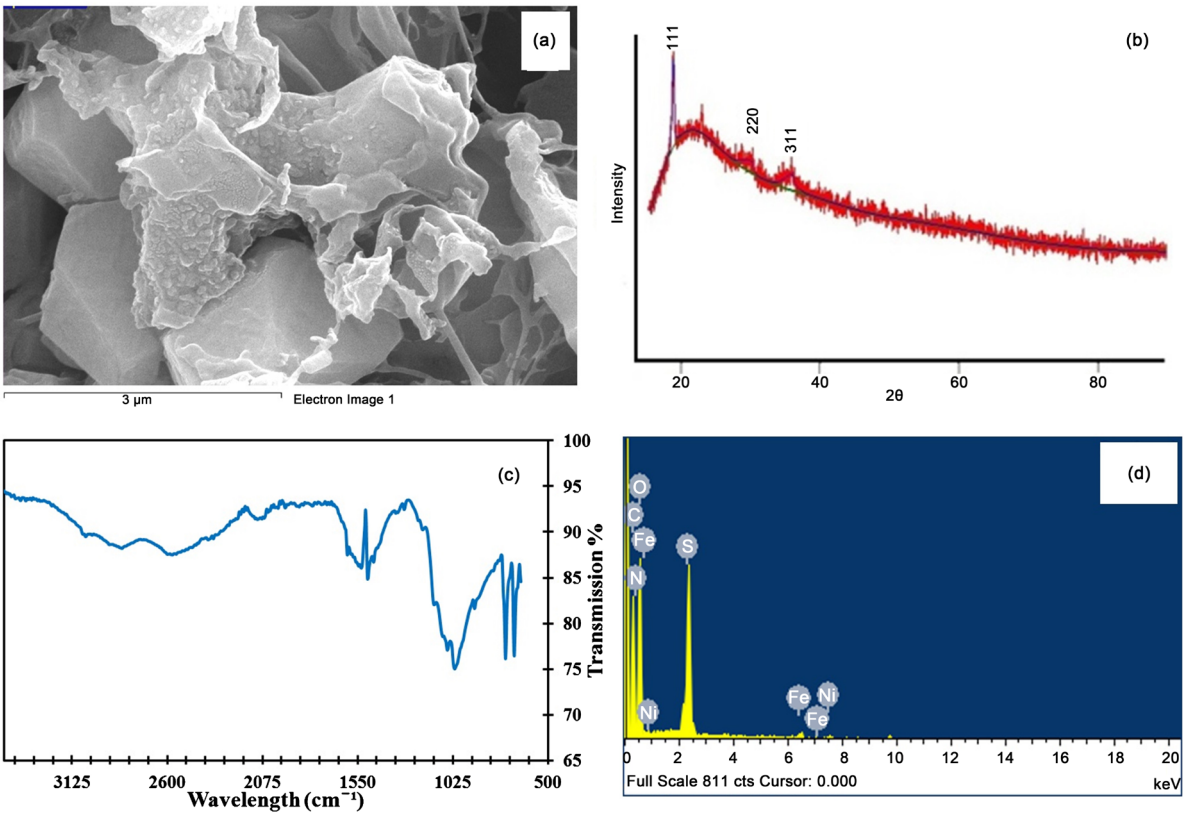

Figure 1. (a) SEM, (b) XRD (c) FTIR, and (d) EDX of PANI/PVA/$NiFe_2O_3$.

Table 1. Elemental analysis of PANI/PVA/$NiFe_2O_3$.

Element	Weight %	Atomic %
C *K*	41.09	51.31
N *K*	4.85	5.20
O *K*	39.88	37.39
S *K*	41.09	51.31
Fe *K*	4.85	5.20
Ni *K*	39.88	37.39
Total	**100%**	

36.01˚ which correspond to the crystal planes of [1, 1, 1], [2, 2, 0] and [3, 1, 1] [14] [16]. This confirmed the crystallinity of the sample which also confirmed by the SEM image in **Figure 1(a)**. The crystallite size of the $NiFe_2O_3$ can be calculated using the Scherrer formula [12]:

$$\tau = \frac{K\lambda}{\beta \cos\theta} \tag{1}$$

where, τ is the mean size of the ordered (crystalline) domains, K is a dimensionless shape factor with a value close to unity, λ is the wavelength and β is the line broadening at half the maximum intensity (FWHM). The average crystallite size is found to be 5.33 nm.

4.2. Electromagnetic Parameter

For the passive medium permittivity and permeability is given by:

$$\epsilon = \epsilon' - i\epsilon'' \tag{2}$$

$$\mu = \mu' - i\mu'' \tag{3}$$

The real part of the permittivity and permeability shows the capacity of storing electric and magnetic energy inside the medium, whereas the imaginary part shows loss inside the material. The microwave absorbing property by the material depends on the dielectric and magnetic loss. **Figure 2(a)** shows frequency dependent of real part and imaginary part of the permittivity. The real part of the permittivity ϵ', has the maximum value of 5.7 (8.2 GHz). As the frequency increases the ϵ' value decreases to 4.95 (12 GHz). The decrease in ϵ' (real part) is due to the decrease in relaxation time of the electric dipole. As PANI is a conducting polymer, electrons can travel freely and accumulate at the interface between $NiFe_2O_3$ and PANI/PVA. Creating a structure similar to a boundary-layer capacitor and generating interfacial dipole polarization. It is found that many hectero-junctions are formed within the polymer composite. In case of the imaginary part of the permittivity the curve is almost linear in the entire frequency. The electrical resonance in the polymer composite may due to space charge polarization and interfacial polarization [17].

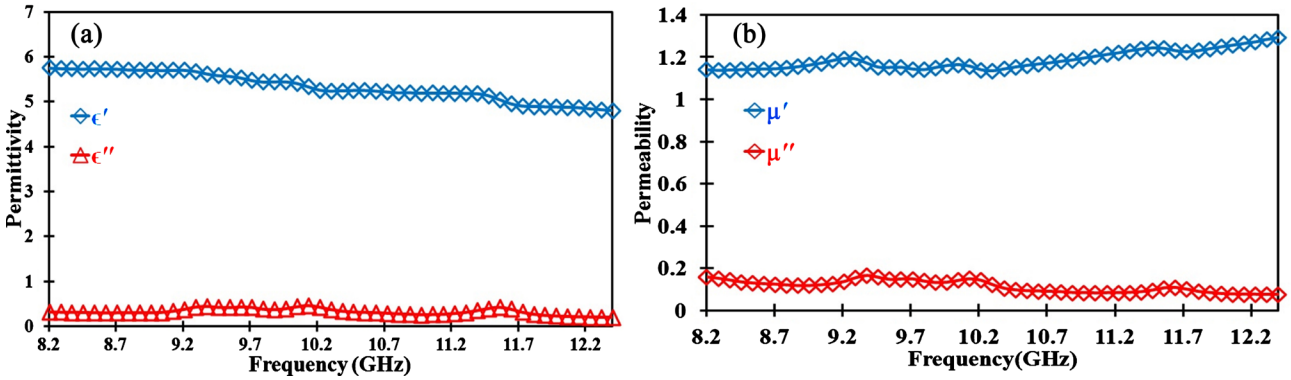

Figure 2. Frequency dependence of (a) permittivity and (b) permeability.

Figure 2(b) shows the frequency dependent of permeability. The value of real part of the permeability increases from 1.14 (8 GHz) to 1.25 (12 GHz) with the increase in frequency. In imaginary part of the permeability decreases from 0.16 (8 GHz) to 0.12 (8.8 GHz) and increases up to maximum of 0.17 (9.45 GHz). The magnetic resonance inside the polymer composite may be due to natural and exchange resonance [11].

Figure 3(a) shows the graph for dielectric and magnetic loss. In our study it is found that the magnetic loss ($\tan\delta_M$) is dominating over the dielectric loss ($\tan\delta_E$). The magnetic loss in the material may be due to the gyromagnetic spin resonance [18]. The dielectric loss inside the material can be explained by the Debye dipole relaxation mechanism. If the plot between the ϵ' and ϵ'' is semi-circle then it is known as Cole-Cole semi-circle given by the relation [19].

$$\left(\epsilon' - \frac{\epsilon_s - \epsilon_\infty}{2}\right)^2 + \left(\epsilon''\right)^2 = \left(\frac{\epsilon_s - \epsilon_\infty}{2}\right)^2 \quad (4)$$

Figure 3(b) shows semi circles representing the two Debye relaxation process. The large number of charge is accumulated at the interface between the $NiFe_2O_3$ and PANI/PVA, which acts like a large electric dipoles which increase the polarization loss [20] [21]. **Figure 3(c)** shows the frequency dependent of impedance. Naturally $NiFe_2O_3$ alone has the high value of the impedance but due to the presence of conducting polymer it has low value of impedance. It has the

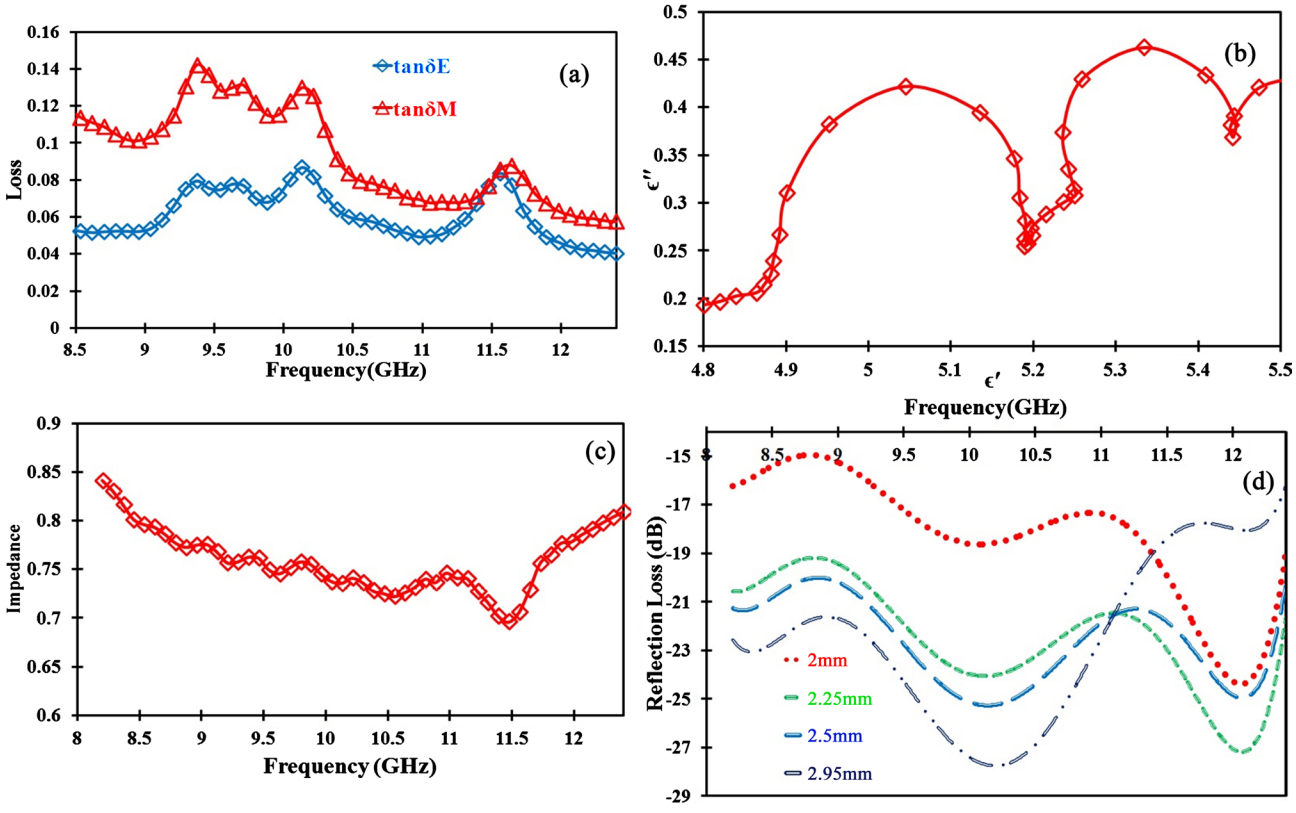

Figure 3. Frequency dependence of (a) dielectric and magnetic loss, (b) between ϵ'' and ϵ', (c) impedance and (d) reflection loss.

maximum value of 0.84 Ω in the lower frequency.

4.3. Reflection Loss Measurement

Reflection loss by the polymer composite is measured by rectangular wave guide method in X-band frequency. The reflection loss measurement with metal back of the material is calculated by using the transmission line theory [22].

$$Z_{in} = Z_0\sqrt{\mu_r/\epsilon_r}\tanh\left[j\left(2\pi fd/c\right)\sqrt{\mu_r\epsilon_r}\right] \quad (5)$$

$$R_L\left(\text{dB}\right) = 20\log\left|\left(Z_{in} - Z_0\right)/\left(Z_{in} + Z_0\right)\right| \quad (6)$$

Here Z_{in} is impedance of the material, Z_0 is the impedance of the free space, μ_r relative permeability, ϵ_r relative permittivity, f frequency, d is the thickness of the sample and R_L is the reflection loss (absorption) by the medium. **Figure 3(d)** shows the microwave reflection losses by the polymer composite. It is found that minimum reflection loss by the polymer composite of thickness 2 mm is −22 dB at the frequency 8.9 GHz which corresponds to 90% absorption of the incident microwave. The minimum reflection for thickness of 2.25 mm, 2.5 mm, 2.95 mm are −27.5 dB (99% at 12 GHz), −25.3 dB (99% at 10.1 GHz), −28 dB (99% at 10.2 GHz) respectively. The absorption is due to the magnetic loss inside the polymer nanocomposite and is confirmed in **Figure 3(a)**. The reflection loss also depends on the surface morphology of the material. The flakes like structure have the minimum reflection loss as compare to the spherical and tube like structure. **Table 2** shows the comparison of reflection loss of our composite along with other reported work.

5. Conclusion

The polymer composite is synthesized by the chemical oxidative polymerization method using APS as the oxidizing agent. The SEM image of the polymer nickel ferrite shows the formation of crystalline structure as supported by the XRD data. The PANI/PVA shows the formation of flake-like structure. The minimum reflection loss (metal back) by the polymer composite is found to be −28 dB with 99% absorbance by the material. Thus this polymer nanocomposite can be used as coating material for adsorbing the microwave frequency between 8 GHz to 12 GHz.

Table 2. Comparison of reflection loss of our polymer composite along with other reported work of same thickness.

Composition	Reflection Loss (dB)	Author
PANI/PVA/$NiFe_2O_3$	−24	Our Work
FeCoB	−12	Zhang *et al.* [23]
Fe_2O_3/PPy	−10	Azadmanjiri *et al.* [24]
Fe_3O_4-3PEDOT	−12	Wencai *et al.* [25]
Fe-Co-Ni	−14.7	Duan *et al.* [26]

Acknowledgements

The authors are thankful to MPCST, Bhopal (Project No. A/RD/RP-2/2013-14/214), Jiwaji University (S. No. /Dev/2016/214) and Post Doctoral Fellowship, Jiwaji University (S. No. F/Dev./2019/611, 2019) for providing research grant, DMSRDE Kanpur for microwave studies, CEERI-Pilani and Central Facility Lab, Jiwaji University, Gwalior for characterization of samples.

Conflicts of Interest

The authors declare no conflicts of interest regarding the publication of this paper.

References

[1] Hermann, D.M. and Hossmann, K.A.J. (1997) Neurological Effects of Microwave Exposure Related to Mobile Communication. *Neurological Sciences*, **152**, 1-14. https://doi.org/10.1016/S0022-510X(97)00140-8

[2] Tiwari, D. C., Jain, R. and Sharma, S. (2008) Spectroscopic and Thermogravimetric Analysis of PANI/PPy Composite Polymer Electrode: Its Application to Electrochemical Investigation of Pharmaceutical Formulation. *Journal of Applied Polymer Science*, **110**, 2328-2336.

[3] Ghanbari, D. and Niasari, M.S. (2015) Synthesis of Urchin-Like CdS-Fe_3O_4 Nanocomposite and Its Application in Flame Retardancy of Magnetic Cellulose Acetate. *Journal of Industrial and Engineering Chemistry*, **24**, 284-292. https://doi.org/10.1016/j.jiec.2014.09.043

[4] Ghanbari, D., Niasari, M.S. and Kooch, M.G. (2014) A Sonochemical Method for Synthesis of Fe_3O_4 Nanoparticles and Thermal Stable PVA-Based Magnetic Nanocomposite. *Journal of Industrial and Engineering Chemistry*, **20**, 3970-3974. https://doi.org/10.1016/j.jiec.2013.12.098

[5] Sobhani, A. and Niasari, M.S. (2015) Synthesis and Characterization of $FeSe_2$ Nanoparticles and $FeSe_2$/FeO(OH) Nanocomposites by Hydrothermal Method. *Journal of Alloys and Compounds*, **625**, 26-33. https://doi.org/10.1016/j.jallcom.2014.11.079

[6] Hashim, M., Alimudin, Kumar, S., Shirsath, S.E., Mohamade, E.D. and Chung, H. (2012) Studies on the Activation Energy from the AC Conductivity Measurements of Rubber Ferrite Composites Containing Manganese Zinc Ferrite. *Physica B*, **407**, 4097-4103. https://doi.org/10.1016/j.physb.2012.06.006

[7] Ajabshir, S.Z., Morassaei, M.S. and Niasar, M.S. (2019) Eco-Friendly Synthesis of $Nd_2Sn_2O_7$-Based Nanostructure Materials Using Grape Juice as Green Fuel as Photocatalyst for the Degradation of Erythrosine. *Composites Part B*: *Engineering*, **167**, 643-653. https://doi.org/10.1016/j.compositesb.2019.03.045

[8] Ajabshir, S.Z. and Niasari, M.S. (2019) Preparation of Magnetically Retrievable $CoFe_2O_4$@SiO_2@$Dy_2Ce_2O_7$ Nanocomposites as Novel Photocatalyst for Highly Efficient Degradation of Organic Contaminants. *Composites Part B*: *Engineering*, **174**, Article ID: 106930. https://doi.org/10.1016/j.compositesb.2019.106930

[9] Abbasi, A., Ghanbari, D., Niasari, M.S. and Hamadanian, M. (2016) Photo-Degradation of Methylene Blue: Photocatalyst and Magnetic Investigation of Fe_2O_3-TiO_2 Nanoparticles and Nanocomposites. *Journal of Materials Science*: *Materials in Electronics*, **27**, 4800-4809. https://doi.org/10.1007/s10854-016-4361-4

[10] Ajabshir, S.Z., Morassaei, M.S. and Niasari, M.S. (2019) Facile Synthesis of $Nd_2Sn_2O_7$-SnO_2 Nanostructures by Novel and Environment-Friendly Approach for the Photodegradation and Removal of Organic Pollutants in Water. *Journal of Environmental Management*, **233**, 107-119. https://doi.org/10.1016/j.jenvman.2018.12.011

[11] Jin, Song, J., Deng, S. and Li, G. (2014) Synthesis and Microwave Absorbing Characteristics of Flake-Like Polypyrrole Filled Composites in X-Band. *Polymer Composite*, **37**, 533-538. https://doi.org/10.1002/pc.23209

[12] Tiwari, D.C., Patil, P.B., Sharma, R., Singh, D. and Singh, S.P. (2007) "Microwave", in Proc. DAE 52th, Solid State Physics, 435-436.

[13] Tiwari, D.C., Dipak, P., Dwevide, S.K., Shami, T.C. and Dwevide, P. (2018) PPy/TiO_2(np)/CNT Polymer Nanocomposite Material for Microwave Absorption. *Journal of Materials Science*: *Materials in Electronics*, **29**, 1643-1650.

[14] Tiwari, D.C., Dipak, P., Dwevide, S.K., Shami, T.C. and Dwivide, P. (2018) Synthesis and Characterization Polymer Nanocomposite of PANI/TiO_2(np)-Fe^{+3} for Microwave Application. *Journal of Materials Science*: *Materials in Electronics*, **29**, 6439-6445. https://doi.org/10.1007/s10854-018-8625-z

[15] Hu, Z.A., *et al.* (2006) The Preparation and Characterization of Quadrate $NiFe_2O_4$/Polyaniline Nanocomposites. *Journal of Materials Science*: *Materials in Electronics*, **17**, 859-863. https://doi.org/10.1007/s10854-006-0042-z

[16] Chauhan, L., Shukla, A.K. and Sreenivas, K. (2015) Dielectric and Magnetic Properties of Nickel Ferrite Ceramics Using Crystalline Powders Derived from DL Alanine Fuel in Sol-Gel Auto-Combustion. *Ceramics International*, **41**, 8341-8351. https://doi.org/10.1016/j.ceramint.2015.03.014

[17] Ma, F., Qin, Y. and Li, Y.Z. (2010) Enhanced Microwave Performance of Cobalt Nanoflakes with Strong Shape Anisotropy. *Applied Physics Letters*, **96**, Article ID: 202507. https://doi.org/10.1063/1.3432441

[18] Zhang, S.Y., Cao, Q.X., Xue, Y.R. and Zhau, Y.X. (2015) Microwave Absorption Performance of the Absorber Based on Epsilon-Fe_3N/Epoxy and Carbonyl Iron/Epoxy Composites. *Journal of Magnetism and Magnetic Materials*, **374**, 755-761. https://doi.org/10.1016/j.jmmm.2014.08.073

[19] Zhang, X.J., Wang, G.S., Wei, Y.Z., Guo, L. and Cao, M.S. (2013) Polymer-Composite with High Dielectric Constant and Enhanced Absorption Properties Based on Graphene-CuS Nanocomposites and Polyvinylidene Fluoride. *Journal of Materials Chemistry A*, **1**, 12115-12122. https://doi.org/10.1039/c3ta12451g

[20] Huang, L., Liu, X., Chuai, D., Chen, Y. and Yu, R. (2016) Flaky FeSiAl Alloy-Carbon Nanotube Composite with Tunable Electromagnetic Properties for Microwave Absorption. *Scientific Reports*, **6**, Article No. 35377. https://doi.org/10.1038/srep35377

[21] Ge, C., Zhang, X., Liu, J., Jin, F., Liu, J. and Bi, H. (2016) Hollow-Spherical Composites of Polyaniline/Cobalt Sulfide/Carbon Nanodots with Enhanced Magnetocapacitance and Electromagnetic Wave Absorption Capabilities. *Applied Surface Science*, **378**, 49-56. https://doi.org/10.1016/j.apsusc.2016.03.210

[22] Matsumoto, M. and Miyata, Y. (1997) Thin Electromagnetic Wave Absorber for Quasi-Microwave Band Containing Aligned Thin Magnetic Metal Particles. *IEEE Transactions on Magnetics*, **33**, 4459-4464. https://doi.org/10.1109/20.649882

[23] Zhang, S.G., Zhu, H.X., Tian, J.J., Pan, D.A., Liu, B. and Kang, Y.T. (2013) Electromagnetic and Microwave Absorbing Properties of FeCoB Powder Composites. *Rare Metals*, **32**, 402-407. https://doi.org/10.1007/s12598-013-0115-0

[24] Azadmanjiri, A., Talemi, P.H., Simon, G.P., Suzuki, K. and Selomulya, C. (2011)

Polymer Engineering & Science, 248-253.

[25] Zhou, W., Hu, X., Sun, C., Yan, J., Zhou, S. and Chen, P. (2014) *Polymers for Advanced Technologies*, **25**, 83-88.

[26] D. Yuping, Z. Yahong, W. Tongmin, G. Shuchao, L. Xin, L. Xingjun, (2014) Evolution Study of Microstructure and Electromagnetic Behaviors of Fe-Co-Ni Alloy with Mechanical Alloying. *Materials Science and Engineering*: *B*, **185**, 86-93. https://doi.org/10.1016/j.mseb.2014.02.014